

Article

Occurrence of State of Gold in Crude Oil and Its Economic Significance

Zhiyong Ni ^{1,2,*} , Wen Zhang ^{1,2}, Jie Liu ^{1,2}, Shengbao Shi ^{1,2}, Xue Wang ^{1,2} and Yang Su ^{1,2}

¹ National Key Laboratory of Petroleum Resources and Engineering, China University of Petroleum (Beijing), Beijing 102249, China; 2023210028@student.cup.edu.cn (W.Z.); mifengguan@outlook.com (J.L.); shengbao@cup.edu.cn (S.S.); 2020010029@student.cup.edu.cn (X.W.); suyangcupb@163.com (Y.S.)

² College of Geosciences, China University of Petroleum (Beijing), Beijing 102249, China

* Correspondence: nizhy@cup.edu.cn

Abstract: Gold and petroleum are also strategic resources of great importance to national security. With the increasing demand for energy, multi-energy cooperative exploration has become an inevitable trend of resource development and utilization. Petroleum and hydrothermal gold deposits may form together, with similar evolutionary trends in their formation, migration, and enrichment. Petroleum reservoirs and gold deposits are closely coupled under certain geological conditions. The solubility of gold in crude oil and its forms of occurrence are important in determining the mechanisms of interaction between gold and petroleum and in facilitating the recovery of gold from gold-bearing petroleum. In this study, the occurrence of gold in crude oil from the Linnan Depression in the Bohai Bay Basin, China, was studied using inductively coupled plasma–mass spectrometry and X-ray photoelectron spectroscopy. Concentrations of gold in crude oil from the Linpan and Shanghe oilfields averaged 44.5 ppb, which is well above the minimum concentration required for hydrothermal gold mineralization. Gold has an affinity with carbon, oxygen, and sulfur, and its concentration in crude oil is positively correlated with total acid and sulfur contents. We speculate that gold may exist in crude oil as complexes with organic acids or thiols, with crude oil thus being a transport medium for gold.

Keywords: crude oil; gold; affinity; organic acid



Citation: Ni, Z.; Zhang, W.; Liu, J.; Shi, S.; Wang, X.; Su, Y. Occurrence of State of Gold in Crude Oil and Its Economic Significance. *Minerals* **2024**, *14*, 351.

<https://doi.org/10.3390/min14040351>

Academic Editor: Jan Golonka

Received: 27 February 2024

Revised: 21 March 2024

Accepted: 27 March 2024

Published: 28 March 2024



Copyright: © 2024 by the authors. Licensee MDPI, Basel, Switzerland. This article is an open access article distributed under the terms and conditions of the Creative Commons Attribution (CC BY) license (<https://creativecommons.org/licenses/by/4.0/>).

1. Introduction

Petroleum and low-temperature hydrothermal Au deposits may form together and exhibit similar evolutionary trends in their formation, migration, and enrichment. Under certain circumstances, oil reservoirs and low-temperature hydrothermal Au deposits, such as Carlin-type deposits, exhibit a close coupling relationship on macro- to micro-scales [1–7] that may manifest in three ways, as follows. (i) Oil and gas reservoirs and Au deposits may have similar spatial distributions. For example, northeastern Nevada, USA, hosts abundant Carlin-type Au deposits and contains numerous oil and gas fields [8,9]; such deposits are also widely developed in the Youjiang Basin, China, together with numerous ancient and residual oil and gas reservoirs [10,11], and many low-temperature hydrothermal Hg, Sb, As, and Au deposits are distributed in the Tongren–Wanshan and Kaili–Majiang–Danzhai paleo-reservoir belts of eastern Guizhou Province, China [12]. (ii) Hydrothermal Au deposits provide records of oil and gas activities. Carlin-type deposits are a type of low-temperature hydrothermal deposit containing ore-bearing rocks that are rich in organic matter, with evidence of organic components participating in mineralization [13]. Liquid hydrocarbon inclusions were found in Carlin-type Au deposits in Nevada, and temperature analyses indicated that the capture temperature of oil-containing inclusions is below 150 °C and within the oil-generation window (80 °C–160 °C) [8,14]. In the Shuiyindong Au mine in the Youjiang Basin, the ore is rich in organic matter and bitumen, and CH₄, CO₂, and N₂ inclusions occur in ore-bearing quartz veins. The sources of these inclusions were linked to

the decomposition of organic matter [15–19]. (iii) Many types of organic matter are enriched in metals. For example, lower Paleozoic dark mudstones of eastern Guizhou, China, are rich in organic C and elements such as Au, V, Ni, and Mo, with metal contents often being positively correlated with total organic C contents. These mudstones are considered “double-source beds” with both mineral and hydrocarbon sources [20,21]. There are also examples of metal-rich bitumen of varying maturity [22]. For example, the Boss deposit in Nevada has a high Au content of 1.3 mg g^{-1} in bitumen within dolomitic limestone. Scanning electron microscopy studies show that Au is present in the bitumen in the form of a Hg alloy $[(\text{Pd}_{81}, \text{Au}_{13}, \text{Pt}_{01}) \text{Hg}]$ [23]. It is possible that metals can be transported in crude oil [24–27]. The contents of Au in the Shengli oilfield, China, are close to the industrial grade of 980 ppb [28], which is several orders of magnitude higher than the average abundance of Au in continental crust (1.8 ppb) [29]. However, there are few examples of the industrial recovery of Au from crude oil worldwide, and there have been no reports of the recovery of Au, Ag, and other precious metals in China because of the difficulty in their recovery [28].

Although many low-temperature hydrothermal Au deposits and oil and gas reservoirs are closely coupled, the mechanisms of ore-formation and oil-accumulation coupling in the interaction between Au and hydrocarbons are poorly understood. Currently, many geologists focus on the role of hydrocarbon fluid in the metallogenic process, the ability to mobilize and transport metal elements, and the metallogenic mechanism of hydrocarbon fluid during basin evolution [3,4,27]. Noble metals such as gold are thought to play a catalytic role in the process of hydrocarbon generation to improve the efficiency of hydrocarbon generation [5]. Petroleum is thought to provide reduced sulfur directly or indirectly for sulfide precipitation during mineralization [1]. It remains unclear whether crude oil can directly participate in the formation of low-temperature hydrothermal Au deposits as a migration medium, but there have been relatively few studies of the contents and forms of Au in crude oil worldwide. This study focused on the Linnan Sag in the Bohai Bay Basin to determine the Au content of crude oil and its form(s) of occurrence. Our results provide insights into the migration of Au in petroleum and its recovery from crude oil.

2. Geological Setting

The Linnan Sag is located in the southwest of Huimin Depression, Bohai Bay Basin, and contains the Linpan oil field, Shanghe oil field, Jiangjiadian oil field, Linan oil field, and so on [30]. The Linnan Sag is controlled by the Linshang and Xiakou Faults on the northern and southern edges, respectively (Figure 1). Xiakou Fault is the most important fault in the Linnan Sag, it controls the distribution of the settlement depocenter and also plays as the channel for petroleum [30].

The Linnan Sag is the main source region of the Huimin Depression, and the distributions of oil fields are mainly demarcated by faults. The Cenozoic tectonic movements of this region include five stages: the initial rifting stage (66.0–46.0 Ma), the intense rifting stage (46.0–38.0 Ma), the shrinking rifting stage (38.0–24.6 Ma), the uplift stage (24.6–14.0 Ma), and the subsiding stage (14.0–0.0 Ma) [30]. There exists an unconformity between the Paleogene and Neogene sequences due to uplift during the Dongying movement (24.6–14.0 Ma). The Cenozoic strata in the Linnan Sag comprise the Paleogene Kongdian Formation (Ek), Shahejie Formation (Es) and Dongying Formation (Ed), the Neogene Guantao Formation (Ng) and Minghuazhen Formation (Nm), and the Quaternary Pingyuan Formation (Qp) [31]. The Ek is dominated by glutenite, sandstone, and siltstone; it formed in a fluvial–lacustrine environment. The Es formation is divided into four parts, which are labeled, respectively, as Es4, Es3, Es2, and Es1 from the bottom to the top, including sandstones and mudstones (Figure 2). The Ng formed in a braided stream environment, including conglomerates, such as sandstones and mudstones. The Nm and Qp are floodplain sediment dominated by mudstones and sandstones [31].

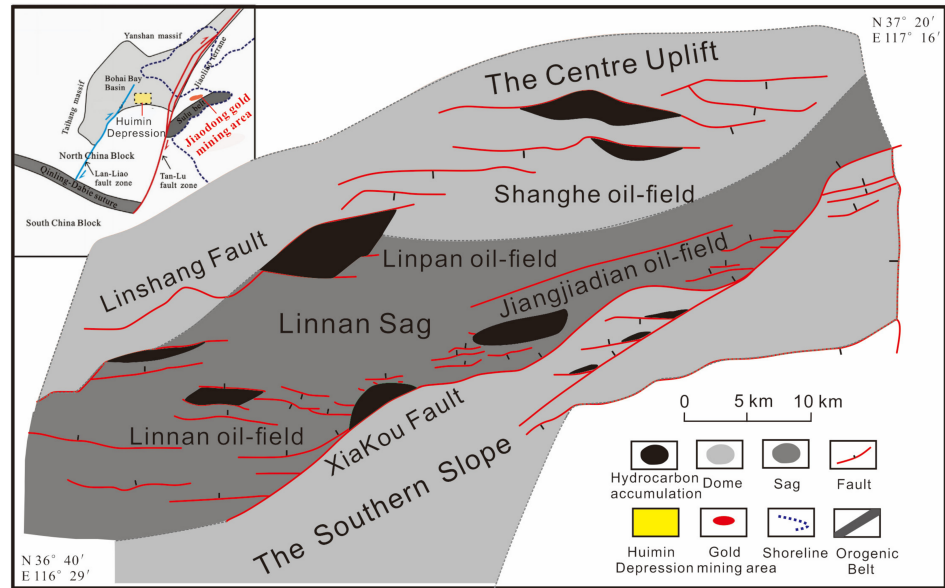


Figure 1. Simplified structural map of the Bohai Bay Basin, sketch map of Linnan Sag and the main oil fields (modified by reference [30]).

System	Series	Stratigraphy			Age (Ma)	Main Source Rocks	Reservoir Rocks	Cap Rocks	Tectonic Evolution	
		Formation	Member	Sub-Member						
Quaternary	Pleistocene	Pingyuan(Qp)								
Neogene	Pliocene	Minghuazhen(Nm)							Subsiding Stage	
		Miocene	Guantao (Ng)	Ng ^u		5.3				
	Ng ^l				14.0					
Paleogene	Oligocene	Dongying (Ed)	Ed ₁		24.6			Shrinking rifting		
			Ed ₂							
			Ed ₃							
	Eocene	Shahejie (Es)	Es ₁			32.8			Syn rift Stage	
			Es ₂							
			Es ₃	Es ₃ ^u		38.0				
				Es ₃ ^m						
				Es ₃ ^l						
			Es ₄	Es ₄ ^u		42.5				
				Es ₄ ^l						
Paleocene	Kongdian (Ek)	Ek ₁			52.0			Initial rifting		
		Ek ₂								
		Ek ₃			66.0					

Figure 2. Schematic Cenozoic stratigraphy and tectonic evolution of the Linnan Sag.

The widely distributed lacustrine mudstones and shales in the lower part of Es3 are the dominant source rocks, with an average total organic carbon content (TOC) of 1.55% [32]. The conglomerate and sandstone in the Es4, Es3, and Es2 are main reservoirs, and Paleogene mudstones are regional cap rocks [32]. It is worth noting that China's famous Jiaodong gold mining area is distributed in the eastern part of the study area (Figure 1).

3. Materials and Methods

Crude oil samples were collected from formations in the Linpan and Shanghe oilfields of the Linnan Sag. The main production beds of crude oil were the Paleogene Shahejie and Neogene Guantao formations. The samples were black solids or viscous semi-solids at room temperature with densities of $>0.86 \text{ g cm}^3$ (i.e., heavy oil).

3.1. Determination of Au Contents

The measurements of elemental analysis were performed at the Analytical Instrumentation Center of Peking University. Microwave digestion and inductively coupled plasma–mass spectrometry (ICP–MS) were employed to determine the Au contents of crude oil. An UltraWAVE ECR (Milestone, Milan, Italy) microwave digestion system was used: 50 mg of crude oil was weighed into a dry digestion tank, 2% HNO_3 was added (1.5 mL), and the sample was sealed and heated to $260 \text{ }^\circ\text{C}$ for 20 min for microwave digestion. The sample was then cooled to below $50 \text{ }^\circ\text{C}$ and transferred to a 30 mL volumetric flask for analysis.

A NexION 350X (PerkinElmer, Waltham, MA, USA) ICP–MS system was used for elemental analysis, with a three-cone interface (sampling, interceptor, over-interceptor cones), a triple four-pole ion deflector, and a universal cell technology with a wide linear range. Working parameters were set by automatic optimization, with a transmission power of 1250 W, carrier-gas flow rate of 0.82 L min^{-1} , peristaltic pump speed of 20.0 rpm, scanning repeated 20 times, and triplicate sample analyses. The standard-addition method was used with internal standards containing Ni, V, and other elements.

3.2. Au-Tube Thermal Simulation

The Au-tube thermal simulation equipment was developed by the State Key Laboratory of Oil and Gas Resources and Exploration, China University of Petroleum (CUP), Beijing, China. Au-tube thermal simulation treatments were undertaken at $420 \text{ }^\circ\text{C}$ and 40 MPa with a reaction time of 72 h. The tube was 60 mm long with an inner diameter of 5.55 mm and a wall thickness of 0.25 mm. A mudstone sample (15 mg of low-maturity source rock from the Bohai Bay Basin) and 160 mg deionized water were placed in the tube, which was sealed by welding in an Ar gas flow. The tube was opened after cooling.

3.3. XPS Analysis

Residual oil on Au-tube surfaces was analyzed by XPS (ThermoFisher, Waltham, MA, USA) at the CUP using Al $K\alpha$ radiation, a spectral range of 0–1100 eV, 20 eV resolution, 0.1 eV step size, and a spot diameter of 300 μm . The instrument etched the Au tube inner surfaces with X-rays for periods of 0, 30, and 60 s, and changes in carbon (C), oxygen (O), nitrogen (N), Sulfur (S), and gold (Au) concentrations with etching depth were recorded. ORIGIN software (OriginPro 2021, 64-bit, 9.8.0.200) was used for graph plotting.

3.4. Determination of Total Acid Values of Crude Oil

The total acid values (TAN) of crude oil samples were determined by acid-base titration (GB/T 264, PRC National Standard) at the CUP [33]. Crude oil samples (2 g) were dissolved in 25 mL of neutral ethanol in a conical flask, and anhydrous ether (25 mL) was added. A blank sample containing 25 mL ethanol and 25 mL ether was also prepared. Phenolphthalein solution (1 mL) was added to each of the mixtures, titration with 0.1 mol L^{-1} KOH was undertaken until the pink endpoint, and the acid value was calculated by $\text{TAN} = (V1 - V2) \times C \times 56.1$, where V1 is the volume of KOH used in sample

titration, V2 is the volume of the KOH solution used in the blank titration, and C is the concentration of the KOH solution.

3.5. The Gas Chromatography–Mass Spectrometry (GC-MS) Analysis

Saturated hydrocarbons of all the crude oils were acquired by standard column liquid chromatography. The GC-MS was performed at the CUP using an Agilent 6890 GC instrument with an Agilent Model 5975i Mass Selective Detector. HP-5 MS fused silica capillary column (30 m × 0.25 mm inner diameter, 0.25 mm thick) was used. The carrier gas was He at constant flow (1 mL/min). The initial GC oven temperature was at 50 °C (held for 1 min) and increased to 100 °C at a rate of 20 °C/min, then ramped to 310 °C at 3 °C/min (held for 10 min).

4. Results

4.1. Crude Oil Au, S, and Total Acid Contents

Twenty-five crude oil samples from the Shahejie and Guantao formations were selected for Au and S analysis; the results are shown in Table 1. Au contents ranged from 12.0 to 107.5 ppb, with an average of 44.5 ppb. S contents ranged from 0.10 to 0.56 wt.% (average 0.32 wt.%). The TAN values ranged from 0.64 to 1.75 mg g⁻¹ (average 1.17 mg g⁻¹).

Table 1. Contents of Au and S and total acid values of crude oil samples.

Oilfield	Well	Fm.	Depth (m)	Density (g/cm ³)	Viscosity (mpa.s)	S (%)	TAN (mg/g)	Au (ppb)
Linpan	L2-x201	G2	1414.4–1423.6	0.945	377.75	0.51	1.63	13.4
Linpan	L23-11	G3	1642.2–1645.0	0.923	90.90	0.37	0.95	105.3
Linpan	L55	S3	2626.6–2992.8	0.866	11.07	0.12	0.92	90.7
Linpan	L7-x28	S2	1799.2–1823.6	0.909	27.46	0.10	0.64	12.0
Linpan	L75-17	S3	1859.2–1909.0	0.918	138.00	0.35	1.11	24.4
Linpan	L75-x30	S4	2474.0–2512.6	0.895	18.00	0.35	1.09	16.0
Linpan	L76-3	S4	2069.0–2094.0	0.893	41.00	0.10	0.82	32.4
Linpan	P14-6	S4	1588.6–1594.4	0.986	5951.00	0.50	1.39	36.6
Linpan	P18-x3	S3	1597.1–1630.3	0.935	119.00	0.42	1.21	38.1
Linpan	P20-6	S1	1556.0–1599.4	0.936	352.30	0.25	1.36	63.1
Linpan	P2-504	S3	1576.0–1606.4	0.965	921.00	0.56	1.21	23.2
Linpan	P40-12	G	1337.6–1354.0	0.960	384.00	0.41	1.49	47.9
Linpan	P40-17	G	1345.4–1350.4	0.951	324.00	0.38	1.33	31.4
Shanghe	S23-70	S2	1710.0–1734.2	0.897	48.94	0.25	0.90	57.2
Shanghe	S25-11	S4	2044.2–2126.8	0.899	48.84	0.14	1.28	18.9
Shanghe	S25-40	S4	1969.6–2267.8	0.897	58.23	0.44	1.21	107.5
Shanghe	S42-2	S2	1655.2–1675.4	0.932	140.30	0.44	0.70	27.3
Shanghe	S70-x5	S2	2348.5–2374.0	0.863	11.26	0.25	1.22	17.5
Shanghe	S73-13	S2	2275.8–2334.2	0.892	40.10	0.37	1.75	34.3
Shanghe	S8-29	S2	1854.2–1859.4	0.887	21.49	0.36	1.52	29.0
Shanghe	S8-300	S2	1776.0–1833.0	0.900	27.90	0.24	0.74	69.0
Shanghe	S8-33	S1	1653.0–1675.0	0.946	322.10	0.50	1.14	83.9
Shanghe	S84-4	S1	1899.0–1903.6	0.872	24.27	0.25	1.31	-
Shanghe	S847	S1	1884.6–1890.4	0.883	29.89	0.17	1.18	41.1
Shanghe	S8-52	S2	1846.0–1861.0	0.897	37.84	0.11	1.15	26.2

4.2. XPS Analyses

After the Au-tube thermal simulation, the tube was cut open to reveal the inner wall covered by generated crude oil. The tube with the most oil was analyzed by XPS, and spectra of Au, C, N, O, and S were recorded for etching times of 0, 30, and 60 s (Figure 3). The double peaks of Au (4f_{5/2} and 4f_{7/2}) were clear, with corresponding binding energies of 82 and 86 eV, respectively. Carbon (1s), N (1s), O (1s), and S (4p_{3/2}) had respective XPS peaks at 283, 398, 530, and 162 eV. Origin software (OriginPro 2021, 64-bit, 9.8.0.200) was

used to process the data, and the results indicate that peak areas of Au, C, and O increased with etching time, whereas that of N decreased (Figure 3, Table 2).

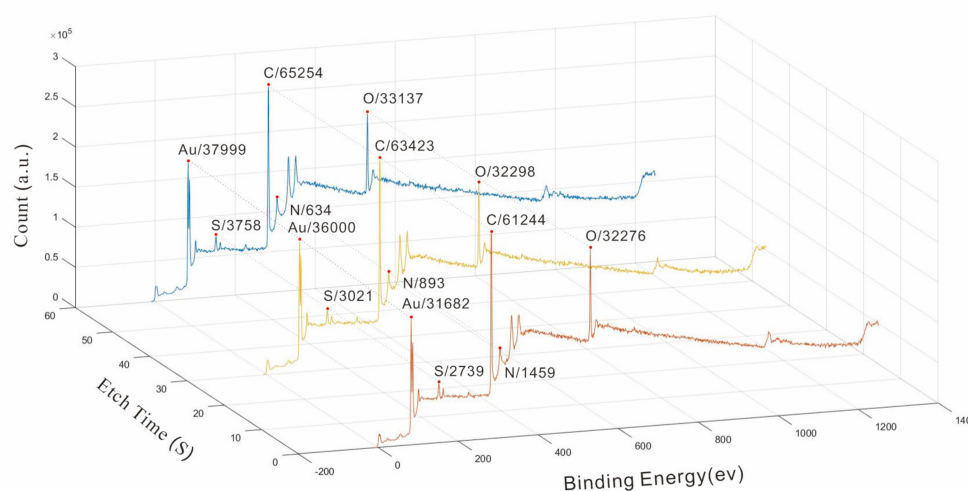


Figure 3. XPS peak areas of Au, C, N, O, and S at etching times of 0, 30, and 60 s.

Table 2. Elemental XPS spectral characteristics.

Elements	Spectral Line	Etch Time (s)	Peak Area	Peak Center (ev)	Elements	Spectral Line	Etch Time (s)	Peak Area	Peak Center (ev)
Au	4f5/2	0	31,682	82	N	1s	0	1459	398
Au	4f5/2	30	36,000	82	N	1s	30	893	398
Au	4f5/2	60	38,000	82	N	1s	60	634	398
Au	4f7/2	0	26,368	86	O	1s	0	32,276	530
Au	4f7/2	30	30,378	86	O	1s	30	32,299	530
Au	4f7/2	60	32,330	86	O	1s	60	33,137	530
C	1s	0	61,244	283	S	4p3/2	0	2739	162
C	2s	30	63,423	283	S	4p3/2	30	3021	162
C	3s	60	65,254	283	S	4p3/2	60	3758	162

5. Discussion

The average Au content of raw oil samples from the Linpan and Shanghe oilfields was 44.5 ppb in our study. However, previous work shows that the maximal Au contents in crude oil samples from the Jiyang Depression, Bohai Bay Basin, can reach 15.74 ppm [34], which is much greater than the industrial Au grade, is typically 0.3–0.5 g tonne⁻¹ (300–500 ppb) [7]. Although the average Au content in our study oil samples is below industrial grade, it may have economic value if an appropriate recovery method is used. The maximal Au concentrations in our oil reached 107.5 ppb at 150 °C, which is considerably higher than the solubility of Au in hydrothermal fluids of the type that have been invoked as possible ore fluids (20 ppb) [20]. The Linpan and Shanghe oilfields are in the Linpan oil-production block, which has an oil-bearing area of 174.6 km² with geological reserves of 283 million tons (Mt) and recoverable reserves of 84 Mt. Based on the average crude oil Au content, the total recoverable Au would be $84 \times 10^6 \times 44.5 \times 10^{-9} = 3.74$ tons, which is equivalent to a small Au mine. Soft/hard acid–base theory [35] implies that Au, as a soft acid, would tend to bind to soft bases such as organic acids and reduced S [36–38]. Previous studies show that there is a strong correlation between the contents of N, O, S, and other heteroatoms and metal elements in crude oil [39,40]. XPS peak areas represent relative contents, and our results (Figure 3) indicate that Au and C peak areas are positively correlated with etching time (i.e., depth), implying a close relationship between Au and organic matter in crude oil. The relative content of O also increased with etching

depth, indicating a further correlation between Au and oxygen contents. Trends in Au, carbon, and oxygen contents were similar, indicating that Au has a strong affinity for C- and O-containing compounds in crude oil. Most O exists as carboxylic acids in crude oil [36]; therefore, Au contents may be closely related to carboxylic acid contents. The relative abundance of S increases with etching depth, and its binding energy corresponds to the XPS peak of Au–thiolate complexes (162.4 eV; Figure 4) [41,42], implying that at least some Au in crude oil may exist in the form of Au thiolate [43,44]. The relative abundance of N decreased with increasing etching depth (Figure 3), indicating no close relationship between Au and nitrogen compounds.

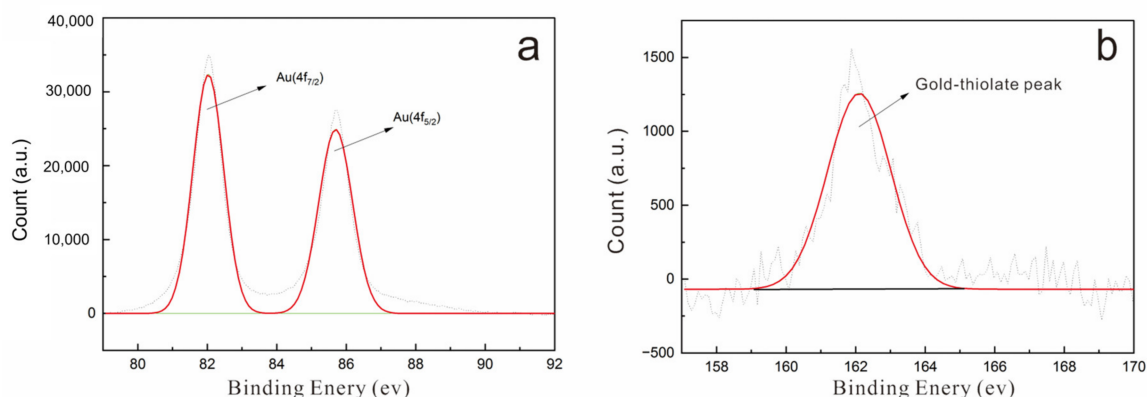


Figure 4. XPS spectra of Au and thiolate (a) the double peaks of Au ($4f_{5/2}$ and $4f_{7/2}$); (b) the peak of Au–thiolate complexes.

To further investigate the occurrence of Au in crude oil, a correlation analysis of Au contents, TAN values, and S contents of 25 crude oil samples was undertaken (Figure 5). When the TAN value was below 1.1, there was a positive correlation between Au content and TAN value; with values above 1.1, there was no obvious correlation. When the oil S content was below 0.35 wt.%, Au contents were positively correlated with S contents but not at higher S contents. The most important determinant of the TAN value of crude oil is the content of organic acids such as carboxylic acid and naphthenic acid [44–46]. Significant quantities of these acids may be released from petroleum source rocks by diffusion during early diagenesis [47]. The investigation shows levels of generation for acetic acid equivalent to 0.2%–1.2% of the TOC of the source rock and total acids at a level of 1%–2% of the TOC [48]. Organic acids are also generally formed by biodegradation as a by-product of bacterial metabolism [49,50]. Similarly, contents of N, O, S, and other heteroatoms may be released from the source rock to oil during the hydrocarbon generation and expulsion process, and the contents of these heteroatoms also increase as crude oil undergoes biodegradation [40,51,52]. Therefore, we speculate that crude oil samples with lower TAN values (<1.1) and S contents (<0.35 wt.%) appear to have a positive correlation with Au contents, which may represent the acid-releasing process from petroleum source rocks by diffusion during early diagenesis. In comparison, crude oil samples with higher TAN values (>1.1) and S contents (>0.35 wt.%) may have been affected by biodegradation, resulting in an insignificant correlation between Au contents and TAN values or S contents. The TAN values and S contents would increase through biodegradation, whereas Au contents would not. This may be due to biodegraded crude oil having a stronger ability to complex Au through its high TAN value and S content, but it would fail to bind more Au owing to its low fluidity. To further verify our speculation about the effect of biodegradation, we performed GC-MS analysis for two typical wells (Well L23-11 and Well P40-17). The total ion current (TIC) diagrams of the saturated hydrocarbons of crude oils from two wells show obviously different degrees of biodegradation. The TIC diagrams of saturated hydrocarbon show that the crude oil from Well L23-11 contains a complete distribution of n-alkane series (Figure 6), which suggests that the crude oil from Well L23-11 did not biodegrade or slightly

biodegrade. By contrast, the TIC diagram of crude oil from Well P40-17 shows an intact n-alkane series and an evident 25-norhopanes, suggesting that the crude oil is a severely biodegraded oil (Figure 6). The results are totally consistent with our speculation based on Figure 5.

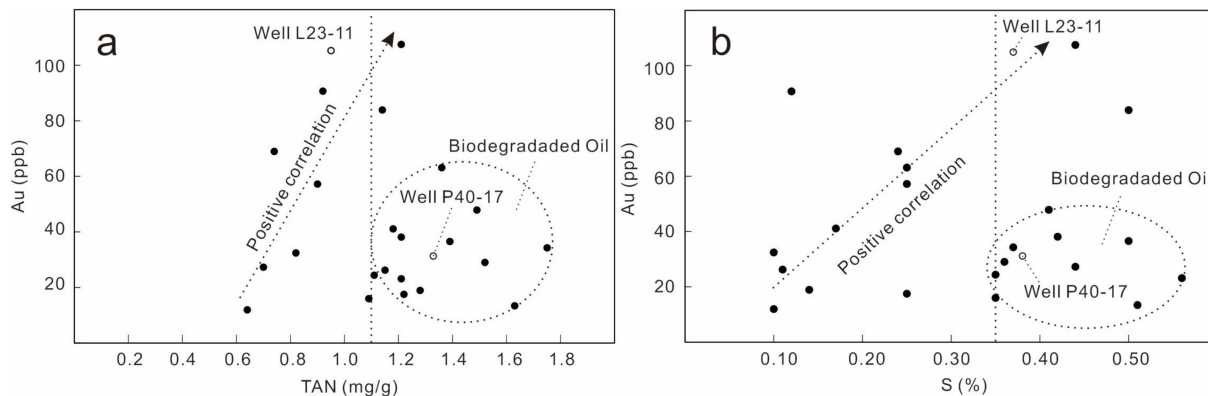


Figure 5. Relationships between crude oil Au contents and (a) total acid (TAN) values and (b) S contents. The arrows indicate the positive correlation between Au and TAN, S; the ellipse regions show that the positive correlations between Au and TAN, S are not obvious; the solid circles denote crude oil samples; the hollow circles denote crude oil samples with GC-MS data.

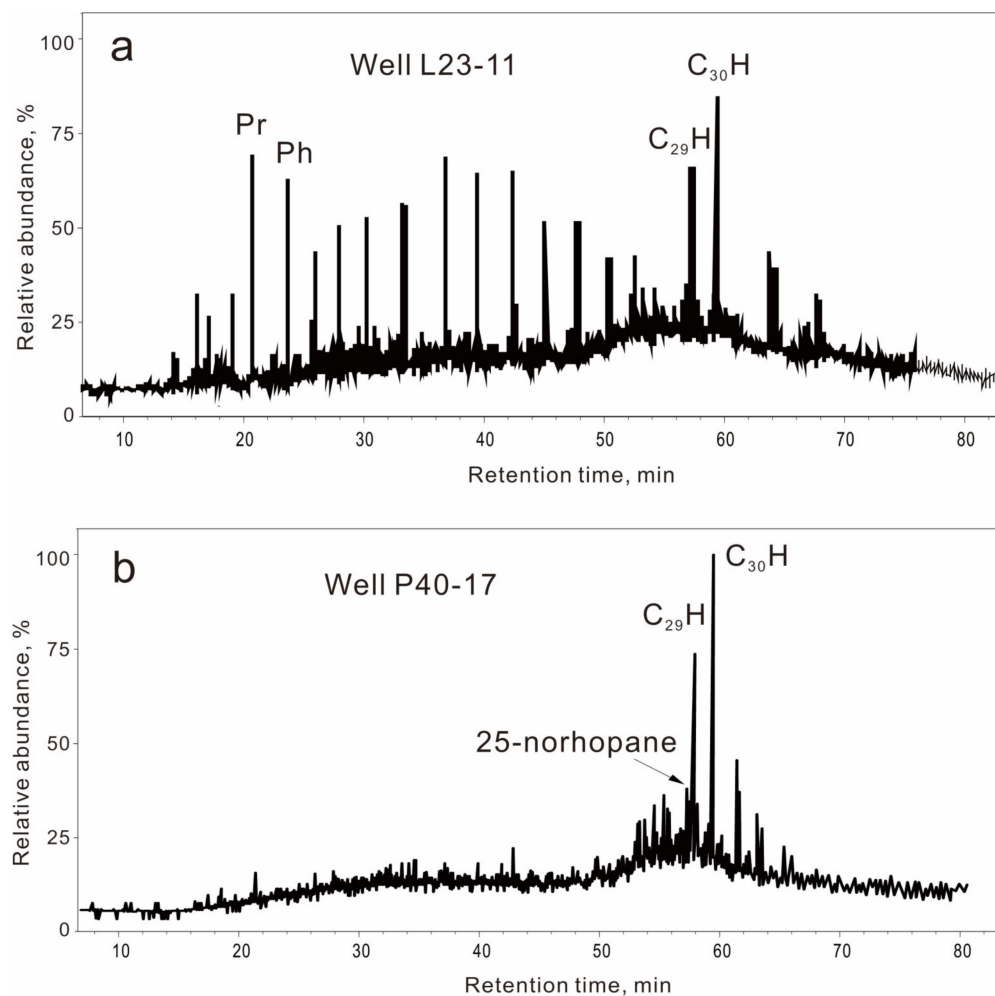


Figure 6. The total ion current diagrams of the saturated hydrocarbons of crude oils. (a) Well L23-11; (b) Well P40-17.

6. Conclusions

The analysis of gold contents of crude oil samples indicates that the gold in oil has economic value if it can be recycled effectively. The possible occurrence states of gold in crude oil are organic acid salts and thiolates. The maximal gold concentrations in our crude oil reached 10.57 ppb, which is considerably higher than the solubility of gold in potential hydrothermal ore-forming fluids. The oil with higher contents of organic acid and sulfur and a lower degree of biodegradation may function as an effective ore-forming fluid for Au deposits.

Author Contributions: Formal data analysis, Z.N., W.Z., J.L., S.S., X.W. and Y.S.; project administration, Z.N.; writing—original draft, Z.N. All authors have read and agreed to the published version of the manuscript.

Funding: This research was funded by the National Natural Science Foundation of China (Grant No. 42273069).

Data Availability Statement: The data presented in this study are available upon request from the corresponding author. The data are not publicly available due to privacy.

Acknowledgments: The help from Wu Jia, Fang Peng and Liang Yun of CUP and Liu Jiahui of Peking University in experiments were acknowledged.

Conflicts of Interest: The authors declare no conflicts of interest.

References

1. Gu, X.X.; Zhang, Y.M.; Li, B.H.; Xue, C.J.; Dong, S.Y.; Fu, S.H.; Cheng, W.B.; Liu, L.; Wu, C.Y. The coupling relationship between metallization and hydrocarbon accumulation in sedimentary basins. *Earth Sci. Front.* **2010**, *17*, 83–105.
2. Clark, J.R.; Williams-Jones, A.E. Analogues of epithermal gold–silver deposition in geothermal well scales. *Nature* **1990**, *346*, 644–645. [[CrossRef](#)]
3. Williams-Jones, A.E.; Migdisov, A.A. An experimental study of the solubility of gold in crude oil: Implications for ore genesis. *Geochim. Cosmochim. Acta* **2006**, *70*, A703. [[CrossRef](#)]
4. Emsbo, P.; Williams-Jones, A.; Koenig, A.E.; Wilson, S.A. Petroleum as an agent of metal transport: Metallogenic and exploration implications. In Proceedings of the Tenth Biennial SGA Meeting, Townsville, Australia, 17–20 August 2009; pp. 99–101.
5. Hu, S.-Y.; Plet, C. Introduction to a special issue on organic- and microbe-metal interactions in mineral systems. *Ore Geol. Rev.* **2022**, *146*, 104938. [[CrossRef](#)]
6. Gu, X.X.; Zhang, Y.M.; Li, B.H.; Dong, S.Y.; Xue, C.J.; Fu, S.H. Hydrocarbon- and ore-bearing basinal fluids: A possible link between gold mineralization and hydrocarbon accumulation in the Youjiang basin, South China. *Miner. Depos.* **2012**, *47*, 663–682. [[CrossRef](#)]
7. Large, R.R.; Bull, S.W.; Maslennikov, V.V. A Carbonaceous Sedimentary Source-Rock Model for Carlin-Type and Orogenic Gold Deposits. *Econ. Geol.* **2011**, *106*, 331–358. [[CrossRef](#)]
8. Hulen, J.B.; Collister, J.W.; Stout, B.; Curtiss, D.K.; Dahdah, N.F. The exhumed “Carlin-type” fossil oil reservoir at Yankee Basin. *JOM* **1998**, *50*, 30–34. [[CrossRef](#)]
9. Collister, J.W.; Hulen, J.B. The oil-bearing, carlin-type gold deposits of Yankee Basin, Alligator Ridge District, Nevada. *Econ. Geol.* **1999**, *94*, 1029–1049.
10. Wang, G.Z.; Hu, R.Z.; Su, W.C.; Zhu, L.M. Fluid and mineralization of Youjiang Basin in the Yunnan-Guizhou-Guangxi area, China. *Sci. China (Ser. D Earth Sci.)* **2002**, *46*, 99–109.
11. Hu, Y.; Liu, W.; Wang, J.; Zhang, G.; Zhou, Z.; Han, R. Basin-scale structure control of Carlin-style gold deposits in central Southwestern Guizhou, China: Insights from seismic reflection profiles and gravity data. *Ore Geol. Rev.* **2017**, *91*, 444–462. [[CrossRef](#)]
12. Hu, Y.Z.; Han, R.S.; Mao, X.X. Relationship between metal mineralization and accumulation oil and gas in the eastern Guizhou. *Geol. Prospect.* **2007**, *43*, 51–56.
13. Arehart, G.B. Characteristics and origin of sediment-hosted disseminated gold deposits: A review. *Ore Geol. Rev.* **1996**, *11*, 383–403. [[CrossRef](#)]
14. Peters, K.E.; Walters, C.C.; Moldowan, J.M. *The Biomarker Guide: Volume 2, Biomarkers and Isotopes in Petroleum Systems and Earth History*; Cambridge University Press: Cambridge, UK, 2007.
15. Su, W.C. Geochemistry of the Ore-Forming Fluids of the Carlin-Type Gold Deposits in the Southwestern Margin of the Yangtze Block. Doctoral Dissertation, Institute of Geochemistry, Chinese Academy of Sciences, Guiyang, China, 2002; pp. 1–120.
16. Xia, Y.; Chen, Q.N.; Zhou, W.C. The simulating experiments of gold mineralization in low temperature and open system. *J. Nanjing Univ. (Nat. Sci.)* **1996**, *32*, 634–639.
17. Liu, J.Z. Ore characteristics and gold occurrence of the Shuiyindong gold deposit, guizhou. *Guizhou Geol.* **2003**, *20*, 30–34.

18. Liu, J.Z.; Deng, Y.M.; Liu, C.Q.; Zhang, X.C.; Xia, Y. Metallogenic conditions and model of the superlarge Shuiyindong stratabound gold deposit in Zhenfeng County, Guizhou Province. *Geol. China* **2006**, *33*, 169–177.
19. Liu, J.Z.; Xia, Y.; Zhang, X.C.; Deng, Y.M.; Su, W.C.; Tao, Y. Model of strata Karlin-type gold deposit: The Shuiyindong super-scale gold deposit. *Gold Sci. Technol.* **2008**, *16*, 1–15.
20. Tu, G.Z. *Geochemistry of Strata-Bound Deposits in China (Volume III)*; Science Press: Beijing, China, 1988.
21. Fu, J.M.; Peng, P.A.; Lin, Q.; Liu, D.H.; Jia, R.F.; Shi, J.X.; Lu, J.L. Several problems in the study of organic geochemistry of strata-bound Deposits. *Prog. Earth Sci.* **1990**, *5*, 43.
22. Parnell, J. Metal enrichments in solid bitumens: A review. *Miner. Depos.* **1988**, *23*, 191–199. [[CrossRef](#)]
23. Jedwab, J.; Badaut, D.; Beaunier, P. Discovery of a palladium-platinum-gold-mercury bitumen in the Boss Mine, Clark County, Nevada. *Econ. Geol.* **1999**, *94*, 1163–1172. [[CrossRef](#)]
24. Baker, W.E. The role of humic acid in the transport of gold. *Geochim. Et Cosmochim. Acta* **1978**, *42*, 645–649. [[CrossRef](#)]
25. Liu, J.Z.; Fu, J.M.; Lu, J.L. Experimental study on the role of organic matter in the mineralization of Sedimentary-reformed gold deposits. *Sci. China (Ser. B)* **1993**, *9*, 993–1000.
26. Zhang, J.R.; Lu, J.J.; Yang, F.; Wu, J.W.; Zhu, F.H. An experimental study on gold solubility in amino acid solution and its geological significance. *Geochimica* **1996**, *25*, 190–195.
27. Crede, L.-S.; Liu, W.; Evans, K.; Rempel, K.; Testemale, D.; Brugger, J. Crude oils as ore fluids: An experimental in-situ XAS study of gold partitioning between brine and organic fluid from 25 to 250 °C. *Geochim. Et Cosmochim. Acta* **2019**, *244*, 352–365. [[CrossRef](#)]
28. Xu, Z.H.; Zhan, Y.L.; Zhu, J.H.; Li, X. The research progress in the utilization of metal resources in crude oils. *Multipurp. Util. Miner. Resour.* **1998**, *3*, 22–26.
29. Taylor, S.R.; McLennan, S.M. *The Continental Crust: Its Composition and Evolution*; Blackwell Scientific Publications: Oxford, UK, 1985.
30. Wang, D.; Wu, Z.P.; Yang, L.L.; Liu, H.; Zhang, Y. Growth and linkage of the Xiakou fault in the Linnan Sag, Jiyang Depression, Eastern China: Formation mechanism and sedimentation response. *Mar. Pet. Geol.* **2020**, *116*, 104319. [[CrossRef](#)]
31. Li, C.; Zhang, L.K.; Luo, X.R.; Wang, B.; Lei, Y.H.; Cheng, M.; Luo, H.M.; Wang, C.J.; Yu, L. Modeling of overpressure generation-evolution of the Paleogene source rock and implications for the Linnan Sag, Eastern China. *Front. Earth Sci.* **2022**, *10*, 829322. [[CrossRef](#)]
32. Guo, X.L.; Xiong, M.; Zhou, Q.; Tian, H.; Xiao, X.M. Petroleum generation and expulsion kinetics: A case study of the Shahejie Formation source rocks from Linnan Sag of Huimin Depression. *ACTA Sedimentol. SINICA* **2009**, *27*, 723–731.
33. GB/T 264-1983; Petroleum Products—Determination of Acid Number. National Bureau of Standards: Beijing, China, 1983.
34. Sun, Y.Z.; Jiao, W.W.; Zhang, S.C.; Qin, S.J. Gold enrichment mechanism in crude oils and source rocks in jiyang depression. *Energy Explor. Exploit.* **2009**, *27*, 133–142. [[CrossRef](#)]
35. Pearson, R.G. Hard and Soft Acids and Bases. *J. Am. Chem. Soc.* **1963**, *85*, 3533–3539. [[CrossRef](#)]
36. Seward, T.M. Thio complexes of gold and the transport of gold in hydrothermal ore solutions. *Geochim. Cosmochim. Acta* **1973**, *37*, 379–399. [[CrossRef](#)]
37. Giordano, T.H. Evaluation of Organic Ligands and Metal-Organic Complexing in Mississippi Valley-Type Ore Solutions. *Econ. Geol.* **1985**, *80*, 96–106. [[CrossRef](#)]
38. Vlassopoulos, D.; Wood, S.A.; Mucci, A. Gold speciation in natural waters: II. The importance of organic complexing- Experiments with some simple model ligands. *Geochim. Cosmochim. Acta* **1990**, *54*, 1575–1586. [[CrossRef](#)]
39. Sanz-Robinson, J.; Williams-Jones, A.E. The solubility of Nickel (Ni) in crude oil at 150, 200 and 250 °C and its application to ore genesis. *Chem. Geol.* **2020**, *533*, 119443. [[CrossRef](#)]
40. Hughey, C.A.; Rodgers, R.P.; Marshall, A.G.; Walters, C.C.; Qian, K.; Mankiewicz, P. Acidic and neutral polar NSO compounds in Smackover oils of different thermal maturity revealed by electrospray high field Fourier transform ion cyclotron resonance mass spectrometry. *Org. Geochem.* **2004**, *35*, 863–880. [[CrossRef](#)]
41. Castner, D.G.; Hinds, K.; Grainger, D.W. X-ray Photoelectron Spectroscopy Sulfur 2p Study of Organic Thiol and Disulfide Binding Interactions with Gold Surfaces. *Langmuir* **1996**, *12*, 5083–5086. [[CrossRef](#)]
42. Sanz-Robinson, J.; Sugiyama, I.; Williams-Jones, A.E. The solubility of palladium (Pd) in crude oil at 150, 200 and 250 °C and its application to ore genesis. *Chem. Geol.* **2020**, *531*, 119320. [[CrossRef](#)]
43. Lewan, M.D. Factors controlling the proportionality of vanadium to nickel in crude oils. *Geochim. Cosmochim. Acta* **1984**, *48*, 2231–2238. [[CrossRef](#)]
44. Giordano, T.H. Metal Transport in Ore Fluids by Organic Ligand Complexation. In *Organic Acids in Geological Processes*; Pittman, E.D., Lewan, M.D., Eds.; Springer: Berlin/Heidelberg, Germany, 1994; pp. 319–354.
45. Speight, J.G. *Handbook of Petroleum Analysis*; John Wiley & Sons Inc: Hoboken, NJ, USA, 2001.
46. Park, L.K.E.; Liu, J.; Yiaccoumi, S.; Borole, A.P.; Tsouris, C. Contribution of acidic components to the total acid number (TAN) of bio-oil. *Fuel* **2017**, *200*, 171–181. [[CrossRef](#)]
47. Lewan, M.D.; Fisher, J.B. Organic Acids from Petroleum Source Rocks. In *Organic Acids in Geological Processes*; Pittman, E.D., Lewan, M.D., Eds.; Springer: Berlin/Heidelberg, Germany, 1994.
48. Barth, T.; Bjørlykke, K. Organic acids from source rock maturation: Generation potentials, transport mechanisms and relevance for mineral diagenesis. *Appl. Geochem.* **1993**, *8*, 325–337. [[CrossRef](#)]

49. Kawamurat, K.; Tannenbaum, E.L.I.; Huizinga, B.J.; Kaplan, I.R. Long-chain carboxylic acids in pyrolysates of Green River kerogen. *Adv. Org. Geochem.* **1986**, *10*, 1059–1065. [[CrossRef](#)]
50. Shock, E.L. Organic acid metastability in sedimentary basins. *Geology* **1988**, *16*, 886–890. [[CrossRef](#)]
51. Head, I.M.; Jones, D.M.; Larter, S.R. Biological activity in the deep subsurface and the origin of heavy oil. *Nature* **2003**, *426*, 344–352. [[CrossRef](#)]
52. Wenger, L.M.; Davis, C.L.; Isaksen, G.H. Multiple Controls on Petroleum Biodegradation and Impact on Oil Quality. *SPE Reserv. Eval. Eng.* **2002**, *5*, 375–383. [[CrossRef](#)]

Disclaimer/Publisher’s Note: The statements, opinions and data contained in all publications are solely those of the individual author(s) and contributor(s) and not of MDPI and/or the editor(s). MDPI and/or the editor(s) disclaim responsibility for any injury to people or property resulting from any ideas, methods, instructions or products referred to in the content.